Continental Climatic and Weathering Response to the Eocene-Oligocene Transition
Author(s): Nathan D. Sheldon, Elisenda Costa, Lluís Cabrera, Miguel Garcés
Reviewed work(s):
Source: *The Journal of Geology*, Vol. 120, No. 2 (March 2012), pp. 227-236
Published by: The University of Chicago Press
Stable URL: http://www.jstor.org/stable/10.1086/663984
Accessed: 06/03/2012 14:08

Continental Climatic and Weathering Response to the Eocene-Oligocene Transition

Nathan D. Sheldon,[1,*] *Elisenda Costa,*[2] *Lluís Cabrera,*[2] *and Miguel Garcés*[2]

1. Department of Geological Sciences, University of Michigan, Ann Arbor, Michigan 48109, U.S.A.;
2. Department of Stratigraphy, Paleontology, and Marine Geosciences, Grup de Geodinàmica i Anàlisi de Conques–GEOMODELS Institute, University of Barcelona, Barcelona, Spain

ABSTRACT

Paleoclimatic reconstructions of the Eocene-Oligocene transition indicate significant spatial heterogeneity in both the marine and the terrestrial responses to the formation of ice sheets on Antarctica. Marine isotopic records indicate that both cooling and ice volume effects contributed to a shift of approximately +1.1‰ in benthic and planktonic foraminiferal $\delta^{18}O$. Because terrestrial records generally are of lower temporal resolution, deconvolving temperature from ice volume effects has been more challenging. New results based on paleosols in a well-dated terrestrial sequence in the Ebro Basin (Spain) bridge this gap by providing a new high-resolution record of paleoclimate and paleoweathering. Between 35 and 33 Ma, the reconstructed mean annual precipitation was unchanged, and mean annual temperatures ranged between ~8° and 14°C, with identical means of ~11°C in both the Eocene and the Oligocene, indicating that paleotemperature was steady in the Ebro Basin. At the same time, a drop in chemical weathering of >30% that was accompanied by a roughly 20% drop in sedimentation rate was observed coincident with declining atmospheric CO_2 levels. Prior to and following the Eocene-Oligocene transition, pedogenic carbonate $\delta^{18}O$ values moved in concert with weathering, but this connection was broken during the Eocene-Oligocene transition itself, suggesting a significant hydrological cycle reorganization at this time. Thus, while the changes in chemical weathering cannot be due to precipitation or temperature changes, the decreased chemical weathering was likely due to falling atmospheric CO_2 levels. This suggests that long-term records of paleosol weathering intensity provide a new proxy for relative atmospheric CO_2 changes.

Online enhancements: appendix tables and figures.

Introduction

The Eocene-Oligocene transition (EOT) was a complex event, with the Antarctic Oi-1 glaciation event known to lag temporally after the Eocene-Oligocene boundary (e.g., Coxall et al. 2005; Pearson et al. 2008) and to have occurred in a series of ice-growth events (Katz et al. 2008) rather than as a single pulse. Although there is some controversy over whether the EOT also required Northern Hemisphere glaciation (Coxall et al. 2005 vs. Liu et al. 2009), there is a strong consensus among marine records (e.g., Zachos et al. 2001; Lear et al. 2008) that there was significant cooling across the EOT. However, the magnitude of the oxygen isotopic shift at and immediately following the EOT requires both changing isotopic composition of seawater associated with the buildup of ice on Antarctica and oceanic temperature change (Zachos et al. 2001; Coxall et al. 2005). In addition, comparison of high- and low-paleolatitude sites indicates regional differences in the magnitude of cooling and of hydrospheric reorganization and seasonality (Eldrett et al. 2009; Liu et al. 2009). Terrestrial records of the EOT also indicate spatial heterogeneity (Sheldon 2009), albeit generally at lower temporal resolution. In addition to a significant mammalian turnover event in Europe that had less impact on other continents ("Grande Coupure"; Hooker et al. 2009; Costa et al. 2011), isotopic proxies based on fossil mammals and invertebrates give contrasting results, with some authors suggesting a significant cooling event (Zanazzi et al. 2007) and others sug-

Manuscript received June 2, 2011; accepted October 17, 2012.
* Author for correspondence; e-mail: nsheldon@umich.edu.

[The Journal of Geology, 2012, volume 120, p. 227–236] 0022-1376/2012/12002-0008$15.00. DOI: 10.1086/663984

gesting stable, unchanging conditions (Kohn et al. 2004; Grimes et al. 2005). Similarly, reconstructions of past precipitation based on paleosols and paleobotanical estimates also come to very different conclusions, with some regions indicating significant aridification at the EOT (Wolfe 1994; Terry 2001; Sheldon and Retallack 2004) and others indicating stability (Eldrett et al. 2009; Sheldon 2009) or even a wetter climate (Sheldon et al. 2009). Here, we present a new high-resolution paleoclimate and paleoweathering intensity record from Ebro Basin (Spain) paleosols of comparable temporal resolution to marine records, which allows us to examine the interplay between paleotemperature and paleohydrology across the EOT.

Geologic Setting

The Ebro Basin (Spain; fig. 1) constitutes the last evolutionary stage of the Pyrenean Foreland Basin, which formed in response to convergence and collision between the Iberian and European plates formed as part of the South Pyrenean foreland basin (e.g., Zoetemeijer et al. 1990). The basin system actively deformed and filled with sediment between the Late Cretaceous and Miocene, transitioning from marine to continental deposition (Busquets et al. 2003). On the basis of mammalian and charophyte biostratigraphy, the continental Artés Formation spans the Upper Eocene to Oligocene (various; e.g., Anadón et al. 1992), and Costa et al. (2010) recently published a high-resolution magnetochronology for it at the paleosol-bearing Maians-Rubió composite section that allows for precise temporal reconstruction of the EOT. The Maians-Rubió section is composed of alluvial and fluvial sediments, with interbedded paleosols (fig. 1; Costa et al. 2010).

Methods

Field Methods and Age Model. Paleosols were identified in the field on the basis of identification of horizonation, root traces/rhizoliths, burrowing, and color and grain size changes (e.g., Terry 2001; Sheldon et al. 2009). Prior to sample collection, 10 cm of lithified surficial material was removed to ensure that the rock samples were not subject to modern alteration. Ages were assigned to individual paleosols using the Gradstein et al. (2004) timescale and are based on the Costa et al. (2010) age model and linear interpolation of sediment accumulation rates for each individual magnetochron. The stratigraphic position of each individual paleosol was recorded relative to the magnetochronology sampling positions (~5 m between paleomagnetic sampling levels), which constrains the precision of the age of an individual paleosol to an average of ± 27.5 k.yr. Work by Costa et al. (2010) indicates that sedimentation rates were generally consistent, although declining slightly, at Maians from 36 to 33 Ma, except for a short-lived rate increase from 35.4 to 35.05 Ma, prior to the paleosol-bearing section (fig. 1) used here to compile the paleoclimatic reconstruction.

Analytical Methods. Fifty-five samples for whole-rock analyses were collected from paleosols at Maians, where 44 of the samples were taken from paleosol B horizons and 11 samples were taken from paleosol A, BC, and C horizons. The samples were analyzed using ICP–optical emission spectrometry and ICP-MS at Royal Holloway, University of London. Analytical uncertainty for major elements was 0.1% and <5 ppm for most trace or rare earth elements.

Pedogenic carbonates were collected from 24 Bk horizons within paleosols at a depth of a minimum of 30 cm beneath the surface of the paleosol to account for diffusive isotope equilibrium and to ensure no atmospheric influence (i.e., below the characteristic production depth of soil CO_2; Cerling 1991). Where profiles were deemed to be complete, the depth to the Bk horizon (which is a function of mean annual precipitation; Retallack 2005) was measured. To avoid potentially diagenetically altered material, carbonate nodules were sawed in half and thin sections made to identify appropriate materials for sampling using a combination of petrographic microscopy and cathodoluminescence; micritic calcite was microdrilled from the second half of the nodules, and samples were analyzed with a MAT253 isotope ratio mass spectrometer connected to a KielIV autosampler device at the University of Michigan. Isotopic results are reported in per mil notation (‰) relative to the Peedee Belemnite standard, and analytical uncertainty was <0.05‰ for both $\delta^{13}C$ and $\delta^{18}O$. Bk depths, whole-rock composition, and isotopic data are provided in the appendix, available in the online edition or from the *Journal of Geology* office.

Climofunction, Weathering, and Provenance Analysis. A variety of tools for quantifying pedogenesis during the formation of a paleosol have been developed that use the chemical composition of either whole profiles or individual horizons (Sheldon and Tabor 2009). For example, one method to assess the provenance/parent material composition of a paleosol is as follows:

$$P = \frac{m_{\mathrm{Ti}}}{m_{\mathrm{Al}}}, \tag{1}$$

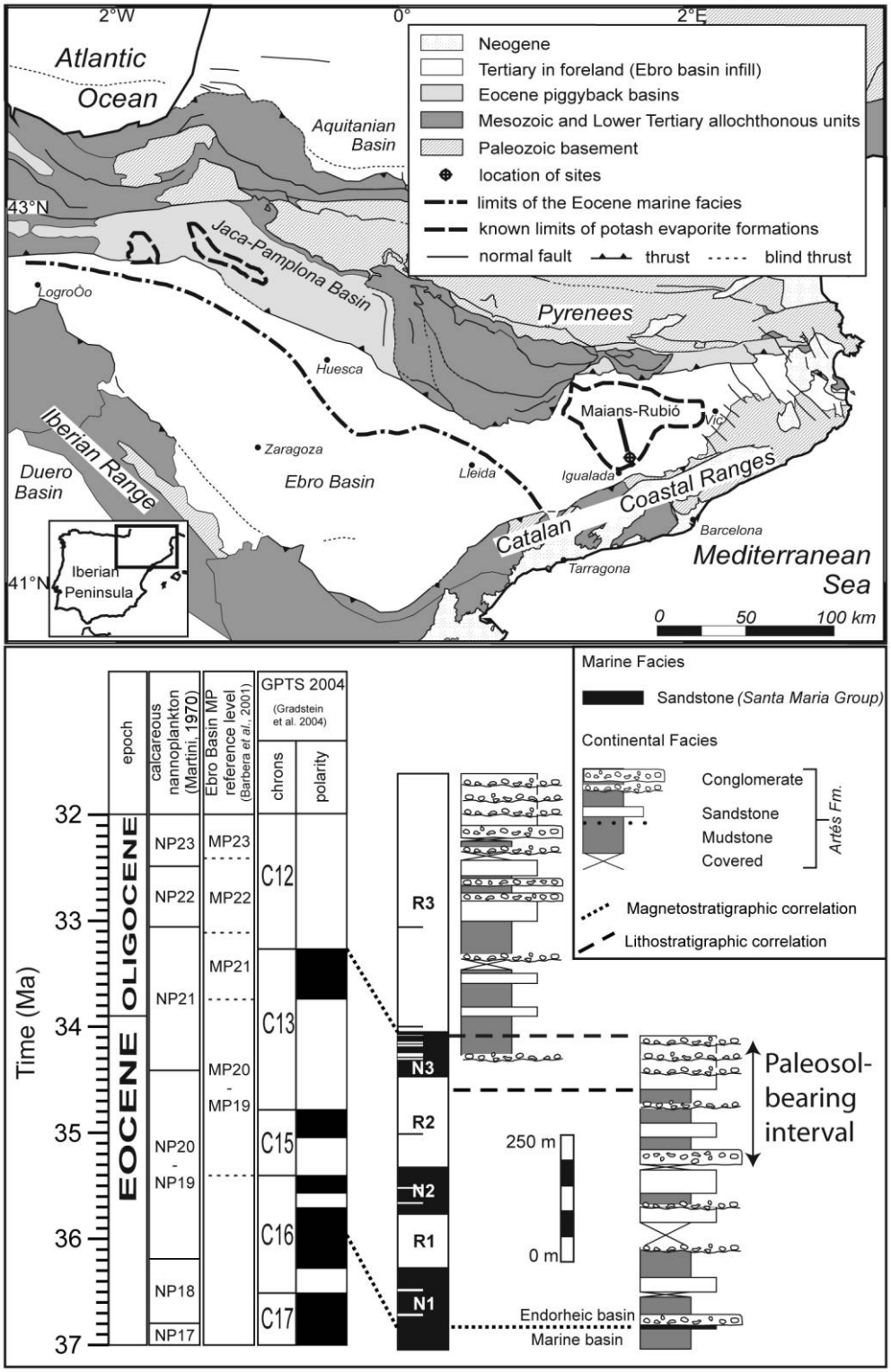

Figure 1. Location map and magnetostratigraphy for the Artés Formation (Ebro Basin, Spain). Both panels are modified from Costa et al. (2010).

where m refers to the molar mass and where values >0.2 are associated with volcanic parent materials and those ≤0.1 are associated with a sedimentary parent (Sheldon and Tabor 2009). Equation (1) has been applied previously to volcanic/volcaniclastic parent materials (e.g., Sheldon 2006), fluvial parent materials (e.g., Hamer et al. 2007*b*), and eolian parent materials (Dal' Bó et al. 2010). Similarly, mean annual temperature (MAT) can be determined by measuring the "clayeyness" (m_{Al}/m_{Si}) of a paleosol's B horizon as follows:

$$T(°C) = 46.9C + 4, \quad (2)$$

where $R^2 = 0.96$ for Inceptisol-like paleosols and the SE on the function is ±0.6°C (Sheldon 2006); including analytical uncertainty and replicate analyses, the total uncertainty is <2°C. Equation (2) has been applied previously to both volcanic/volcaniclastic (e.g., Sheldon 2006; Takeuchi et al. 2007) and fluvial depositional settings (Hamer et al. 2007*a*, 2007*b*). If it can be demonstrated that there is no change in the provenance of paleosol parent material (eq. [1]), then long-term changes in chemical weathering (ΔW) can be assessed as follows:

$$\Delta W = \mathrm{CIA}_x - \mu_{\mathrm{CIA}}, \quad (3)$$

where CIA refers to the chemical index of alteration (Nesbitt and Young 1982) of a given paleosol's B horizon (x) or the mean (μ) for that time period (Sheldon and Tabor 2009).

Calculated results from eqq. (2) and (3) are plotted as five-point running averages in figures 2 and 3. Both calculated values for individual paleosols and those from the smoothed running averages are compiled in the appendix.

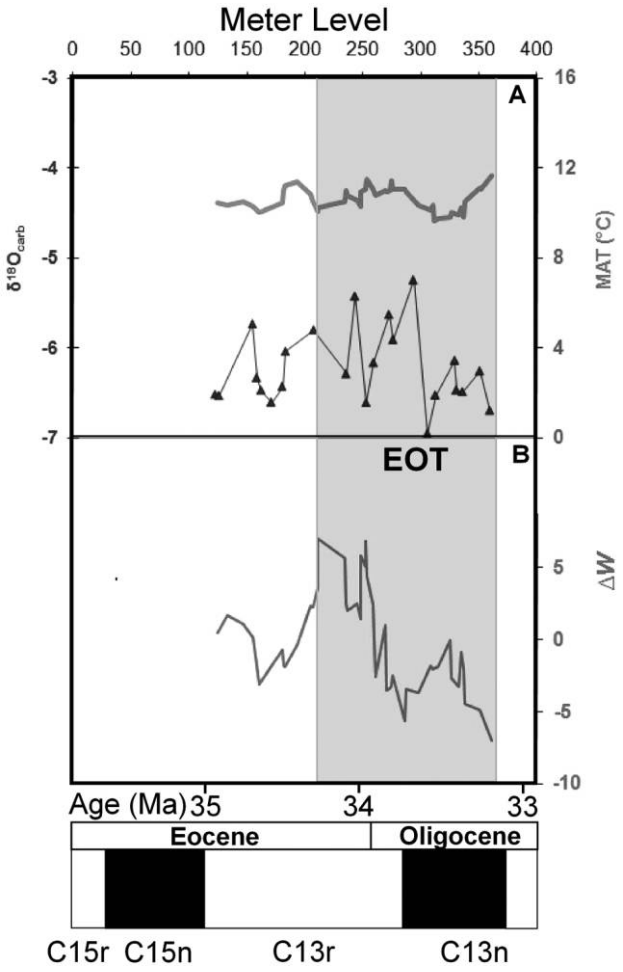

Figure 2. Paleoclimatic proxies spanning the Eocene-Oligocene transition (EOT) in the Ebro Basin, Spain. The shaded area represents the EOT. *A*, Mean annual temperature (MAT; from paleosol chemistry) and pedogenic carbonate $\delta^{18}O$, where the MAT is plotted as a five-point running average; the SE for the MAT estimate is ±0.6°C (total uncertainty is less than ±2°C), and the analytical uncertainty for the $\delta^{18}O$ analyses is less than the size of the data points. *B*, Chemical weathering (ΔW) spanning the Eocene-Oligocene transition in the Ebro Basin, Spain, plotted as a five-point running average. Absolute ages were determined as described in "Methods," and are all given according to the Gradstein et al. (2004) timescale. A color version of this figure is available in the online edition of the *Journal of Geology*.

Results

Paleosol Taxonomy. On the basis of USDA taxonomy (Soil Survey Staff 1999), the paleosols preserved at Maians are either weakly developed Entisol-like paleosols with A-C profiles or weakly to moderately developed Inceptisol-like paleosols with A-Bw-(Bk)-C profiles (fig. A1, available online or from the *Journal of Geology* office), which makes the use of equation (2) appropriate for reconstructing MAT rather than some of the other proxies that have been developed (Sheldon et al. 2002). Entisol-like paleosols cannot be used to constrain paleoclimatic conditions. Typical pedogenic features observed include centimeter-scale burrows; taxonomically diagnostic horizons, including Bw and Bk horizons; color changes throughout the profiles; rare redoximorphic features; rhizoliths; and rare casts of terrestrial invertebrates (fig. A1). Although there is little functional difference between the two systems, some paleosol workers prefer to use the paleosol-specific taxonomic scheme of Mack et al. (1993) rather than the USDA scheme, which includes some specific secondary and tertiary taxonomic criteria that are not typically preserved in

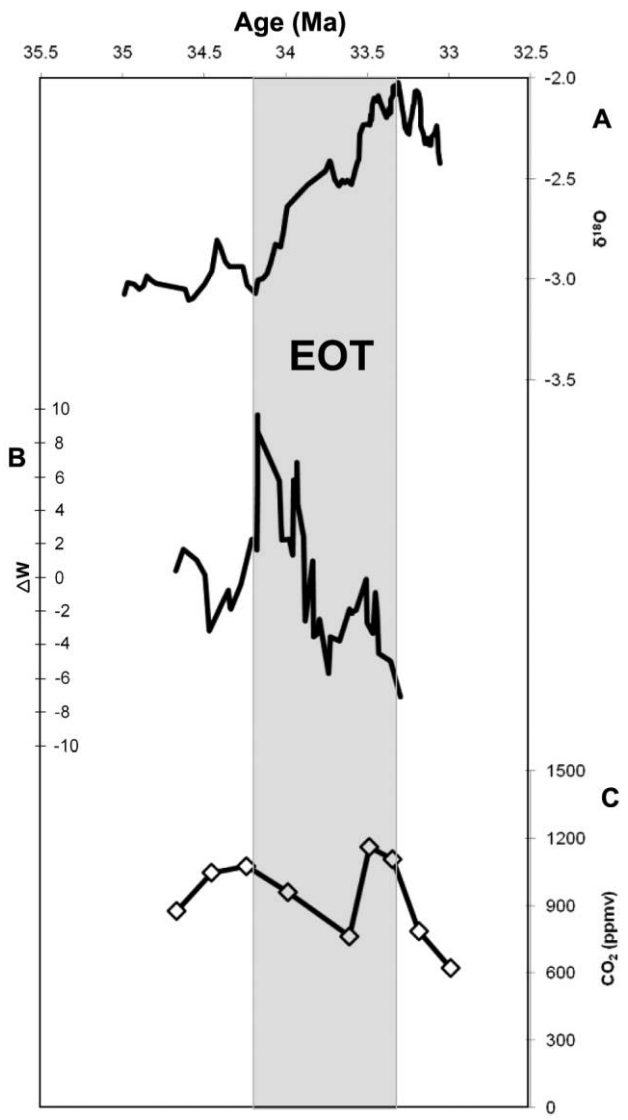

Figure 3. Comparison between the Ebro Basin weathering (ΔW) record and marine records of the Eocene-Oligocene transition (EOT). *A*, Five-point running average of marine planktonic $\delta^{18}O$ values from Pearson et al. (2008). *B*, ΔW record from the Ebro Basin, plotted as a five-point running average. *C*, Atmospheric P_{CO_2} estimates based on $^{11}B/^{10}B$ isotopes; data are from Pearson et al. (2009). Both the marine $\delta^{18}O$ and paleosol ΔW records show a two-step change across the EOT. Data in *A* and *C* use the Berggren and Pearson (2005) timescale, which places the Eocene-Oligocene boundary at 33.7 Ma, whereas *B* uses the Gradstein et al. (2004) timescale, which revised the age of the boundary to 33.9 Ma. Data are plotted according to the absolute ages for each timescale, and regardless of the precise age of the Eocene-Oligocene boundary, the EOT spans time before and after either boundary pick.

paleosols. Applying the Mack et al. (1993) scheme, all the profiles would key out either as Calcisols if there is a Bk horizon present or as Protosols if no Bk horizon is present. Measured Bk depths (n = 9) for complete, uneroded paleosols ranged between 35 and 60 cm (mean = ~ 51 cm), with no significant difference between the mean Eocene (51.4 ± 9.0 cm) and Oligocene (47.5 ± 3.5 cm) Bk depths. For the purposes of comparison between the taxonomic schemes, Protosol may apply to either Entisol-like or Inceptisol-like paleosols and Calcisol refers only to the Inceptisol-like paleosols, but regardless of taxonomy only the moderately developed paleosols are appropriate for paleoclimatic reconstruction.

Whole-Rock Geochemistry. When equation (1) is used, the Ti/Al ratio is unchanged throughout the whole section, with a mean of 0.066 for both the Eocene and the Oligocene paleosols (see fig. A2, available online or from the *Journal of Geology* office), which indicates that there was no change in source material through time and that all the paleosols had a sedimentary protolith (Sheldon and Tabor 2009). Given that the paleosols key out as Inceptisol-like, equation (2) may be used to calculate MAT. The mean calculated MAT (fig. 2*A*) for the Eocene (n = 24) is 10.9° ± 1.4°C (1σ). The mean calculated MAT for the Oligocene (n = 20) is 10.6° ± 1.5°C (1σ). Again, the values are statistically indistinguishable. The mean calculated ΔW (fig. 2*B*) for the Eocene paleosols is 1.8, which is 12.6% higher than the mean CIA for the whole interval (14.3). The mean calculated ΔW for the Oligocene paleosols is −3.2, which is 22.7% lower than the mean CIA for the whole interval. Thus, there is a significant reduction in chemical weathering across the EOT (fig. 2).

Stable Isotope Geochemistry. Pedogenic carbonate nodules from Maians are 66.8%–90.8% carbonate by weight, with a mean of 80.8%, which represents relatively pure carbonate for a pedogenic system. Carbonate $\delta^{13}C$ values range between −4.23‰ and −6.09‰, with an Eocene mean of −5.12‰ ± 0.60‰ (1σ) and a statistically indistinguishable Oligocene mean of −4.74‰ ± 0.42‰ (1σ; not shown). Carbonate $\delta^{18}O$ values range between −5.24‰ and −6.95‰, with an Eocene mean of −6.23‰ ± 0.37‰ (1σ) and a statistically indistinguishable Oligocene mean of −6.23‰ ± 0.52‰ (1σ; fig. 2*A*). There was no relationship between pedogenic carbonate $\delta^{13}C$ and $\delta^{18}O$ values (R^2 = 0.02; fig. A3, available online or from the *Journal of Geology* office), so diagenetic alteration of the samples is unlikely (Sheldon and Tabor 2009).

Discussion

Comparison to Other Continental Records. Sheldon (2009) compared a number of paleosol-bearing sections that span the EOT and noted that there is a broad range in the continental response to global cooling and drying associated with the EOT (table 1). The Ebro Basin EOT record is most similar to that of Montana (Sheldon and Retallack 2004; Retallack 2007), which also indicates no significant cooling or drying and shares a similar physiographic setting (endorheic basin). In contrast, the climatic response of sites closer to coastal areas (Oregon and Isle of Wight) is stronger, indicating a more significant connection between marine and terrestrial depositional systems in those settings; however, none of the continental paleosol records indicate a large magnitude cooling event (table 1). Records of $\delta^{18}O$ from vertebrates are also regionally variable—tooth enamel $\delta^{18}O$ from specimens spanning the EOT in Argentina indicates climatic stability (Kohn et al. 2004), whereas a fossil bone diagenesis $\delta^{18}O$ record from Nebraska stands as an outlier relative to other continental records and to the paleosol record from the same site in indicating a significant cooling event (table 1; Zanazzi et al. 2007). As Sheldon (2009) noted, the most likely explanation for the discrepancy is that a significant part of the $\delta^{18}O$ shift was a result of regional aridification that has been consistently reconstructed by various workers (Terry 2001; Sheldon and Retallack 2004; Retallack 2007), a factor that was not accounted for by Zanazzi et al. (2007), who interpreted the isotopic shift entirely in terms of temperature. That interpretation is also inconsistent with marine records that indicate changing ocean $\delta^{18}O$ as a function of both temperature and ice volume (Liu et al. 2009).

Comparison to Marine Records. Recent high-resolution marine $\delta^{18}O$ records (Coxall et al. 2005; Katz et al. 2008; Pearson et al. 2008) of paleoclimatic change across the EOT indicate that it was a more complex event, characterized by a series of small stepwise changes, than suggested by older, lower-resolution marine records (Zachos et al. 2001), which appeared to indicate a monotonic change. Sea-surface temperature reconstructions based on $U^{K'}_{37}$ and TEX_{86} records also indicate significant differences between high- and low-latitude marine responses to the EOT, with very little cooling at low-latitude sites and a cooling of ~5°C at high (>45°N or S) paleolatitudes (Liu et al. 2009). This significant equator-pole gradient in sea-surface temperatures should also have resulted in differences in continental moisture ability as a function of latitude.

Figure 3 shows a comparison between the high-resolution marine planktonic $\delta^{18}O$ record from the Tanzania Drilling Project (Pearson et al. 2008) and the Ebro Basin ΔW record. The shift to more positive $\delta^{18}O$ values is thought to be driven by a combination of climatic cooling and ice-sheet growth (e.g., Zachos et al. 2001), which impacts both oceanic salinity and moisture availability for the continents. The ΔW record indicates a significant drop in chemical weathering across the EOT, with peak weathering intensity at the onset of the event dropping to the lowest values of the whole data set at the end of the record. The onset of the EOT in both records is essentially simultaneous within the errors of the respective age models, and both records show a stepwise change consistent with other marine records, including benthic foraminiferal records (Coxall et al. 2005; Katz et al. 2008). This similarity is consistent with a single driving mechanism for the changes observed in all of the records, which is mostly likely Antarctic ice-sheet growth and hydrospheric reorganization triggered by falling atmospheric P_{CO_2} levels (fig. 3; DeConto et al. 2008; Pearson et al. 2009).

Climatic or Hydrospheric Change across the EOT? The total range of reconstructed MAT (see the appendix) fluctuates between 8° and 14°C during the

Table 1. Continental Eocene-Oligocene Transition Boundary Sites Compared

Locality[a]	Mean annual precipitation	Mean annual temperature
Argentina	NA	Unchanged
Ebro Basin (Spain)	Unchanged	Unchanged
Isle of Wight (England)	Wetter	Unchanged
Montana	Unchanged	Unchanged
Nebraska	Dryer	Cooler (<2°C paleosols; 8°C vertebrates)
Oregon	Dryer	Cooler (<2°C)

Note. NA = not available (results not reported).

[a] Results are based on (*a*) vertebrates (Argentina [Kohn et al. 2004] and Zanazzi et al. 2007) and (*b*) paleosols (Ebro Basin [this study], Isle of Wight [Sheldon et al. 2009], and Montana, Nebraska, and Oregon [Sheldon and Retallack 2004; Retallack 2007]).

EOT, but there is no significant trend and no evidence of an either unidirectional single or multistep cooling event. Instead, the mean MAT and range of reconstructed MAT values are indistinguishable between the Eocene and the Oligocene (fig. 2), suggesting that there was no significant cooling event locally in the Ebro Basin during the EOT. Although it represents a significantly smaller data set than the other proxies, on the basis of the Bk depths of nine uneroded paleosols (Eocene = 7, Oligocene = 2) there is no significant change in mean annual precipitation across the EOT in the Ebro Basin either (see the appendix).

There was a significant drop in chemical weathering across the EOT, as indicated by the drop in ΔW values in a gross sense (mean Eocene vs. mean Oligocene) as well as temporally associated with the EOT interval itself (fig. 2*B*, 3). The drop in ΔW is accompanied by a gradual reduction in sedimentation rate over the period of the record, from 201 m m.yr.$^{-1}$ during 35.05–34.75 Ma to 163 m m.yr.$^{-1}$ during 33.73–33.25 Ma (Costa et al. 2010). Thus, the ~30% reduction in chemical weathering as measured by ΔW is accompanied by an ~20% reduction in sedimentation rate. All the paleosols used to construct the curve are Inceptisol-like paleosols, which should have formed in a comparable amount of time on the basis of their degree of development (e.g., Sheldon and Tabor 2009) and consistent carbonate nodule size (<2 cm; Retallack 2005), so the changing ΔW values cannot be explained in terms of duration of pedogenesis. There are three possibilities that could explain the EOT shift: (1) change in the composition of material being weathered, (2) change in atmospheric P_{CO_2}, and (3) reorganization of the hydrosphere (e.g., changing seasonality). The first explanation can be discounted because there is no change in provenance of the materials that are being weathered, so figure 2*B* represents weathering intensity.

Given the apparent stability in MAP indicated by paleosol Bk depth measurements, declining weathering intensity could be due to declining atmospheric P_{CO_2} levels (fig. 3). This idea is supported by a number of proxies. For example, alkenone (Pagani et al. 2005), stomatal index data (Retallack 2002), and boron isotope data (Pearson et al. 2009) indicate significantly elevated P_{CO_2} in the Eocene relative to the Oligocene, and a sharp drop in atmospheric P_{CO_2} across the EOT has been implicated in triggering the growth of ice sheets in Antarctica (DeConto et al. 2008). Similar MAP but lower atmospheric P_{CO_2} (and, therefore, higher raindrop pH) would lead to less intense weathering given that there is no evidence of changing plant communities during the EOT (Hooker et al. 1995). For example, on the basis of thermodynamic data from Holland and Powell (1998) and a temperature of 10°C (consistent with the paleosol data herein; fig. 2), the pH of a raindrop at the low end of Pearson et al.'s (2009) P_{CO_2} reconstruction (i.e., 600 ppmv) would be 5.49, whereas for the high end of their reconstruction (i.e., 1200 ppmv) the pH would be 5.34. Although that difference may seem relatively small, biotic responses to ocean acidification (e.g., calcification) are detectable at even more modest pH changes (Orr et al. 2005; Ries et al. 2009), and plants are also known to be impacted by rain pH (various; e.g., Shepherd and Griffiths 2006; Kovacik et al. 2011). Thus, declining ΔW across the EOT is consistent with declining atmospheric P_{CO_2} levels.

It is significant to note that prior to and following the EOT the ΔW and $\delta^{18}O$ records (fig. 2) generally move in phase with one another but respond in opposite ways to the EOT itself. While the mean pedogenic $\delta^{18}O$ is statistically indistinguishable between the Eocene and the Oligocene, the signal is relatively volatile, with a difference of up to ~1.7‰ over a short time interval, and becomes episodically significantly heavier during the EOT itself (fig. 2*a*), which could indicate either a significant cooling or a significant change in the composition of the meteoric water source from which the carbonates precipitated. Given that there is no local temperature change indicated by the paleosol MAT record and no significant change in local precipitation abundance indicated by the Bk depth record, the second explanation best explains the data. Previous work at the nearby (relatively) Isle of Wight EOT succession (Grimes et al. 2005) and at North Atlantic Ocean Drilling Program EOT sites (Liu et al. 2009) is also consistent with a shift in the meteoric water composition rather than a temperature-only response. The positive $\delta^{18}O$ shifts in the pedogenic carbonates during the EOT (fig. 2*A*) are consistent with a heavier local oceanic source (e.g., Katz et al. 2008) for meteoric water derived from the North Atlantic that fluctuates through time. In contrast to marine records (fig. 3), the pedogenic carbonate $\delta^{18}O$ (fig. 2*A*) record does not establish a new baseline after the initiation of the Oi-1 event (~33.5 m.yr. ago) but instead continues to be volatile, although with smaller magnitude changes than before the EOT. This also coincides with a second drop in chemical weathering (figs. 2*B*, 3) and, temporally, with the main Oi-1 event (e.g., Katz et al. 2008). Taken together, the various lines of evidence suggest that significant hydrosphere reorganization occurred

during the EOT because the strong connection between $\delta^{18}O$ and ΔW prior to and following the EOT is lost during the EOT.

Conclusions

On the basis of multiple proxies, there was no significant cooling or drying locally in the Ebro Basin during the EOT. At the same time, the EOT itself is characterized by intermittently heavier $\delta^{18}O$ values for meteoric water, consistent with ice-sheet growth, and by a >30% decline in chemical weathering intensity, consistent with falling atmospheric P_{CO_2}. The ΔW record indicates a multistep decline in chemical weathering that corresponds very well temporally with multistep marine $\delta^{18}O$ records, suggesting common causal mechanisms. Prior to the EOT, changes in the pedogenic $\delta^{18}O$ and ΔW records from the Ebro Basin were generally in phase, suggesting a connection between the seasonal availability of water and weathering intensity, but this connection was lost during the EOT itself. A second drop in chemical weathering coincident with the Oi-1 event accompanied by lower amplitude fluctuations in $\delta^{18}O$ values suggests that Antarctic glaciations led to a significant reorganization of the hydrosphere in the Northern Hemisphere.

The strong relationship between ΔW and marine $\delta^{18}O$ and CO_2 reconstructions suggests that this new proxy may provide a valuable means of relating both the timing of climatic changes in marine and continental records and the relative intensity of change. Potentially, then, this could provide a new proxy for changes in atmospheric CO_2 levels.

ACKNOWLEDGMENTS

We thank two anonymous reviewers and the Editor (D. Rowley) for constructive comments that improved the manuscript. N.D.S. was supported by a Strategic Research Fund grant from Royal Holloway, University of London, during his time there. E.C. was supported by a Formación de Personal Investigador grant from the Spanish Ministerio de Ciencia e Innovación (MCI). This article was developed within the framework of the Spanish MCI projects CENOCRON CGL2004-00780 and REMOSS 3D-4D CGL2007-66431-C02-02/BTE and is a contribution of the Grup de Geodinàmica i Anàlisi de Conques (2009 GGR 1198, Comissionat d'Universitats i Recerca de la Generalitat de Catalunya) and the GEOMODELS Institute.

REFERENCES CITED

Anadón, P.; Cabrera, L.; Choi, S. J.; Colombo, F.; Feist, M.; and Saéz, A. 1992. Biozonación del Paleógeno continental de la zona oriental de la Cuenca del Ebro mediante carófitas: implicaciones en la biozonación general de carófitas de Europa occidental. Acta Geol. Hisp. 27:69–94.

Barberá, X.; Cabrera, L.; Marzo, M.; Parés, J. M.; and Agustí, J. 2001. A complete terrestrial Oligocene magnetostratigraphy from the Ebro Basin, Spain. Earth Planet. Sci. Lett. 187:1–16.

Berggren, W. A., and Pearson, P. A. 2005. A revised tropical to subtropical Paleogene planktonic foraminiferal zonation. J. Foraminifer. Res. 35:279–298.

Busquets, P.; Serra-Kiel, J.; and Ferràndez-Cañadell, C. 2003. New advances in Eocene Biostratigraphy (IGCP Project n° 393): a contribution from the Southeastern Pyrenean Foreland Basin—volume in honour of Professor Salvador Reguant. Geol. Acta 1(2):151–238.

Costa, E.; Garcés, M.; López-Blanco, M.; Beamud, E.; Gómez-Paccard, M.; and Larrasoaña, J. C. 2010. Closing and continentalization of the South Pyrenean foreland basin (NE Spain): magnetochronological constraints. Basin Res. 22:904–917.

Costa, E.; Garcés, M.; Sáez, A.; Cabrera, L.; and López-Blanco, M. 2011. The age of the "Grande Coupure" mammal turnover: new constraints from the Eocene-Oligocene record of the Eastern Ebro Basin (NE Spain). Palaeogeogr. Palaeoclimatol. Palaeoecol. 301: 97–107.

Coxall, H. K.; Wilson, P. A.; Palike, H.; Lear, C. H.; and Backman, J. 2005. Rapid stepwise onset of Antarctic glaciation and deeper calcite compensation in the Pacific Ocean. Nature 433:53–57.

Dal' Bó, P. F. F.; Basilici, G.; and Angelica, R. S. 2010. Factors of paleosol formation in a Late Cretaceous eolian sand sheet paleoenvironment, Marília Formation, southeaster Brazil. Palaeogeogr. Palaeoclimatol. Palaeoecol. 292:349–365.

DeConto, R. M.; Pollard, D.; Wilson, P. A.; Pälike, H.; Lear, C. H.; and Pagani, M. 2008. Thresholds for Cenozoic bipolar glaciations. Nature 455:652–656.

Eldrett, J. S.; Greenwood, D. R.; Harding, I. C.; and Huber, M. 2009. Increased seasonality through the Eocene to Oligocene transition in northern high latitudes. Nature 459:969–973.

Gradstein, F. M.; Ogg, J.; and Smith, A. 2004. A geologic time scale 2004. Cambridge, Cambridge University Press.

Grimes, S. T.; Hooker, J. J.; Collinson, M. E.; and Mattey, D. P. 2005. Summer temperatures of Late Eocene to Early Oligocene freshwaters. Geology 33:189–192.

Hamer, J. M. M.; Sheldon, N. D.; and Nichols, G. J. 2007*a*. Global aridity during the Early Miocene? a terrestrial paleoclimate record from the Ebro Basin, Spain. J. Geol. 115:601–608.

Hamer, J. M. M.; Sheldon, N. D.; Nichols, G. J.; and Collinson, M. E. 2007*b*. Late Oligocene–Early Miocene paleosols of distal fluvial systems, Ebro Basin, Spain. Palaeogeogr. Palaeoclimatol. Palaeoecol. 247: 220–235.

Holland, T., and Powell, R. 1998. An internally consistent thermodynamic dataset for phases of petrological interest. J. Metamorph. Geol. 16:309–343.

Hooker, J. J.; Collinson, M. E.; Van Bergen, P. F.; Singer, R. L.; De Leeuw, J. W.; and Jones, T. P. 1995. Reconstruction of land and freshwater palaeoenvironments near the Eocene-Oligocene boundary, southern England. J. Geol. Soc. Lond. 152:449–468.

Hooker, J. J.; Grimes, S. T.; Mattey, D. P.; Collinson, M. E.; Sheldon, N. D. 2009. Refined correlation of the UK Late Eocene–Early Oligocene Solent Group and timing of its climate history. *In* Koeberl, C., and Montanari, A., eds. The Late Eocene Earth: hothouse, icehouse, and impacts. Geol. Soc. Am. Spec. Pap. 452:179–195.

Katz, M. E.; Miller, K. G.; Wright, J. D.; Wade, B. S.; Browning, J. V.; Cramer, B. S.; and Rosenthal, Y. 2008. Stepwise transition from the Eocene greenhouse to the Oligocene icehouse. Nat. Geosci. 1:329–334.

Kohn, M. J.; Josef, J. A.; Madden, R.; Vucetich, G.; and Carlini, A. A. 2004. Climate stability across the Eocene-Oligocene transition, southern Argentina. Geology 32:621–624.

Kovacik, J.; Klejdus, B.; Backor, M.; Stork, F.; and Hedbavny, J. 2011. Physiological responses of root-less epiphytic plants to acid rain. Ecotoxicology 20:348–357.

Lear, C. H.; Bailey, T. R.; Pearson, P. N.; Coxall, H. K.; and Rosenthal, Y. 2008. Cooling and ice growth across the Eocene-Oligocene transition. Geology 36: 251–254.

Liu, Z. H.; Pagani, M.; Zinniker, D.; DeConto, R.; Huber, M.; Brinkhuis, H.; Shah, S. R.; Leckie, R. M.; and Pearson, A. 2009. Global cooling during the Eocene-Oligocene climate transition. Science 323: 1187–1190.

Nesbitt, H. W., and Young, G. M. 1982. Early Proterozoic climates and plate motions inferred from major element chemistry of lutites. Nature 299:715–717.

Mack, G. H.; James, W. C.; and Monger, H. C. 1993. Classification of paleosols. Geol. Soc. Am. Bull. 105: 129–136.

Martini, E. 1970. Standard Palaeogene calcareous nannoplankton zonation. Nature 226:560–561.

Orr, J. C.; Fabry, V. J.; Aumont, O.; Bopp, L.; Doney, S. C.; Feely, R. A.; Gnanadesikan, A.; et al. 2005. Anthropogenic ocean acidification over the twenty-first century and its impact on calcifying organisms. Nature 437:681–686.

Pagani, M.; Zachos, J. C.; Freeman, K. H.; Tipple, B.; and Bohaty, S. 2005. Marked decline in atmospheric carbon dioxide concentrations during the Paleogene. Science 309:600–603.

Pearson, P. N.; Foster, G. L.; and Wade, B. S. 2009. Atmospheric carbon dioxide through the Eocene-Oligocene climate transition. Nature 461:1110–1113.

Pearson, P. N.; McMillan, I. K.; Wade, B. S.; Jones, T. D.; Coxall, H. K.; Bown, P. R.; and Lear, C. H. 2008. Extinction and environmental change across the Eocene-Oligocene boundary in Tanzania. Geology 36:179–182.

Retallack, G. J. 2002. Carbon dioxide and climate over the past 300 Myr. Philos. Trans. R. Soc. A 360:659–673.

———. 2005. Pedogenic carbonate proxies for amount and seasonality of precipitation in paleosols. Geology 33:333–336.

———. 2007. Cenozoic paleoclimate on land in North America. J. Geol. 115:271–294.

Ries, J. B.; Cohen, A. L.; and McCorkle, D. C. 2009. Marine calcifers exhibit mixed responses to CO_2 induced ocean acidification. Geology 37:1131–1134.

Sheldon, N. D. 2006. Quaternary glacial-interglacial climate cycles in Hawaii. J. Geol. 114:367–376.

———. 2009. Non-marine records of climatic change across the Eocene-Oligocene transition. *In* Koeberl, C., and Montanari, A., eds. The Late Eocene Earth: hothouse, icehouse, and impacts. Geol. Soc. Am. Spec. Pap. 452:241–248.

Sheldon, N. D.; Mitchell, R. L.; Collinson, M. E.; and Hooker, J. J. 2009. Eocene-Oligocene transition paleoclimate record from paleosols, Isle of Wight (UK). *In* Koeberl, C., and Montanari, A., eds. The Late Eocene Earth: hothouse, icehouse, and impacts. Geol. Soc. Am. Spec. Pap. 452:249–260.

Sheldon, N. D., and Retallack, G. J. 2004. Regional precipitation records from the late Eocene and early Oligocene of North America. J. Geol. 112:487–494.

Sheldon, N. D.; Retallack, G. J.; and Tanaka, S. 2002. Geochemical climofunctions from North American soils and application to paleosols across the Eocene-Oligocene boundary in Oregon. J. Geol. 110:687–696.

Sheldon, N. D., and Tabor, N. J. 2009. Quantitative paleoenvironmental and paleoclimatic reconstruction using paleosols. Earth-Sci. Rev. 95:1–52.

Shepherd, T., and Griffiths, D. W. 2006. The effects of stress on plant cuticular waxes. New Phytologist 171: 469–499.

Soil Survey Staff. 1999. Keys to soil taxonomy (8th edition). Blacksburg, VA, USDA Natural Resources Conservation Service, 600 p.

Takeuchi, A.; Larson, P. B.; and Suzuki, K. 2007. Influence of paleorelief on the Mid-Miocene climate variation in southeastern Washington, northeastern Oregon, and western Idaho, USA. Palaeogeogr. Palaeoclimatol. Palaeoecol. 168:462–476.

Terry, D. O. 2001. Paleopedology of the Chardron Formation, northwestern Nebraska: implications for paleoclimate in the North American mid-continent

across the Eocene-Oligocene boundary. Palaeogeogr. Palaeoclimatol. Palaeoecol. 168:1–39.

Wolfe, J. A. 1994. Tertiary climatic changes at middle latitudes of western North America. Palaeogeogr. Palaeoclimatol. Palaeoecol. 108:195–205.

Zachos, J.; Pagani, M.; Sloan, L.; Thomas, E.; and Billups, K. 2001. Trends, rhythms, and aberrations in global climate 65 Ma to present. Science 292:686-693.

Zanazzi, A.; Kohn, M. J.; McFadden, B. J.; and Terry, D. T. 2007. Large temperature drop across the Eocene-Oligocene transition in central North America. Nature 445:639–642.

Zoetemeijer, R.; Desegaulx, P.; Cloetingh, S.; Roure, F.; and Moretti, I. 1990. Lithospheric dynamics and tectonic-stratigraphic evolution of the Ebro Basin. J. Geophys. Res. 95:2701–2711.